acta phys. slov. 43 (1993), No. 4, 243–270

OPTIMAL SYSTEMATICS OF SINGLE-HUMPED FISSION BARRIERS FOR STATISTICAL CALCULATIONS

S.G. Mashnik [1]

Laboratory of Theoretical Physics, Joint Institute for Nuclear Research, Dubna, Head Post Office, P.O.B. 79, 101000 Moscow, Russia

Received 5 February 1993; in final form 5 April 1993
Accepted 15 April 1993

A systematic review and comparison of the existing phenomenological approaches and models for fast calculations of single-humped fission barriers is given. The effects of angular momentum and excitation energy dependence of fission barriers are discussed. Experimental data on excitation energy dependence of the fissility Γ_f/Γ_{tot} of compound nuclei are analyzed in the framework of the statistical approach by using different models for fission barriers, shell and pairing corrections and level density parameter in order to identify their reliability and range of applicability for Monte Carlo calculations of evaporative cascades. The energy dependence of fission cross-sections for reactions induced by intermediate energy protons has been analyzed in the framework of the Cascade-Exciton Model. A proposal for measurements at the FOBOS setup at Joint Inst. Nucl. Res. is given.

I. INTRODUCTION

The statics of fission is governed by the variation of the potential energy of a fissioning system as a function of deformation in the transition from the initial state to scission (see recent reviews [1]-[5]). Therefore, the most important characteristics of fissioning nuclei are fission barriers determined as differences between the saddle-point and ground state masses

$$B_f = M_{sp}(A,Z) - M_{gs}(A,Z)\ . \tag{1}$$

Various models used to calculate B_f can be classified in three categories: microscopic, semiclassical or hybrid, and macroscopic ones (see [5] for a review). In microscopic models, the nucleus is studied as a many-body problem of an ensemble of nucleons moving in a self-consistent Hartree-Fock field with possible extensions (see, e.g., [6]). This method should provide accurate knowledge of the fissioning system. However, the complexity of the effective nucleon-nucleon interaction as

[1] E-mail address: MASHNIK@THEOR.JINRC.DUBNA.SU

well as the great number of nucleons in a heavy nucleus make the calculations very difficult and too lengthy to be used in Monte Carlo calculations of competing fission and evaporation processes. Therefore, for statistical applications, the "regular" part of fission barriers is usually calculated either in the framework of such macroscopic approaches as different versions of liquid-drop model (LDM) [7]-[9], droplet model [11, 12], single-Yukawa modified LDM [13], Yukawa-plus-exponential modified LDM [10, 14, 15], or phenomenologically approximated [16] in accordance with their experimental values.

To estimate the "irregular" microscopic part of B_f, different hybrid approaches are used taking into account quantal corrections for shell and pairing effects, finite range of the nuclear force, effects of the diffuseness of the nuclear surface and other physics effects [7]-[14]; or various phenomenological approximations are used [16, 17]. Apparently, the most adequate description of macroscopic fission barriers for hot and usually rotating nuclei has been done by Sierk [15]. Sierk also performed a global fit for macroscopic part of B_f for nuclei with their atomic numbers from 20 to 100 for the entire range of the angular momentum L for which a fission barrier exists and he obtained a global representation of results which depends only on three variables: A, Z and L. This global approximation is provided as Fortran-77 subroutine BARFIT (see [15]) and it may be easily incorporated in the statistical evaporation model calculations. But this code may require too much computing time to obtain a satisfactorily statistics in the Monte Carlo simulation of reactions in some cases.

In the present work we compare different approaches and models for fission barriers that are easy to be computed. This is done in order to find out their applicability for statistical calculations of nuclear reactions involving fission processes.

II. MACROSCOPIC-MICROSCOPIC APPROACHES TO FISSION-BARRIER HEIGHTS

In the hybrid macroscopic-microscopic approach, a fission barrier is given by a sum of a macroscopic smooth term and a microscopic term, each of them being in the general case a function of the charge Z and the atomic mass number A, the excitation energy of the fissioning nucleus E^*, its angular momentum L and deformation α

$$B_f(A,Z,E^*,L,\alpha) = B_f^{macro}(A,Z,E^*,L,\alpha) + B_f^{micro}(A,Z,E^*,L,\alpha). \quad (2)$$

As the starting point of our cosiderations, we do not take into account the excitation energy and angular momentum dependences of B_f.

BITG73 approximation

Barashenkov *et al.* [16] has proposed to use a simple phenomenological approximation for fission barriers in fast statistical calculations. The authors of [16] suggested not to calculate fission barriers within Monte Carlo simulations of nuclear reactions, but to use known experimental values and to extract from them the

phenomenological "irregular" part which depends on shell corrections, residual interactions and other nuclear structure effects, and by approximating the remaining "regular" part by a simple analytical expression

$$B_f^{BITG73}(A,Z) = B_f^0(A,Z) - \delta W_{gs}^{BITG73}(A,Z) + \delta W_{sp}^{BITG73}(A,Z). \quad (3)$$

The "regular" part of the experimental fission barriers $B_f^0(A,Z)$ was well approximated by the function (in MeV)

$$B_f^0(A,Z) = 12.5 + \begin{cases} +4.7(33.5 - Z^2/A)^{3/4}, & \text{if } Z^2/A \le 33.5\ ; \\ -2.7(33.5 - Z^2/A)^{2/3}, & \text{if } Z^2/A > 33.5\ . \end{cases} \quad (4)$$

The "irregular" part was divided into two terms: a correction to the nuclear ground state mass $\delta W_{gs}^{BITG73}(A,Z)$ and a correction to the nuclear saddle-point mass $\delta W_{sp}^{BITG73}(A,Z)$. The use of the Cameron shell and pairing corrections tabulated in [18] has been proposed for $\delta W_{gs}^{BITG73}(A,Z)$ [16]

$$\begin{aligned} \delta W_{gs}^{BITG73}(A,Z) &= \Delta(Z,N) = S(Z,N) + P(Z,N) \equiv \\ &\equiv [S(Z) + P(Z)] + [S(N) + P(N)]; \quad (N = A - Z)\ . \end{aligned} \quad (5)$$

Alternatively, data on

$$\Delta(Z,N) = S(Z) + P(Z) + S(N) + P(N), \quad (6)$$

tabulated in a subsequent work by Cameron *et al.* [19] are very convenient for numerical calculations of evaporative cascade.

In Fig. 1, these two sets of Cameron's shell corrections are shown for a collection of odd-odd nuclei together with the Myers and Swiatecki LDM shell corrections [7]. One can see that the discrepancy in the absolute values of two sets of Cameron's shell corrections is small (it is close to 2 MeV for just a few nuclei), while the discrepancy between Cameron's and Myers and Swiatecki's values is more significant. The approximation

$$\delta W_{sp}^{BITG73}(A,Z) = \left\{ \begin{matrix} \text{-0.5 for even } Z \\ \text{0 for odd } Z \end{matrix} \right\} + \left\{ \begin{matrix} \text{0 for even } N \\ \text{1 for odd } N \end{matrix} \right\}. \quad (7)$$

(in MeV) was obtained for $\delta W_{sp}^{BITG73}(A,Z)$.

BG77 approximation

Another simple semi-phenomenological approximation for fission barriers has been proposed by Barashenkov and Gereghi [17]. They use formula analogous to (3) to calculate fission barriers

$$B_f^{BG77}(A,Z) = B_f^0(Z^2/A) - \Delta(A,Z) + \delta^{BG77}(A,Z). \quad (8)$$

It was proposed to use the same Cameron's corrections (5) or (6) for $\Delta(A,Z)$, while

$$\delta^{BG77}(A,Z) = \begin{cases} 0, & \text{for even } Z \text{ and even } N\ ; \\ \delta_f, & \text{for odd } A\ ; \\ 2\delta_f, & \text{for odd } Z \text{ and odd } N\ ; \end{cases} \quad (9)$$

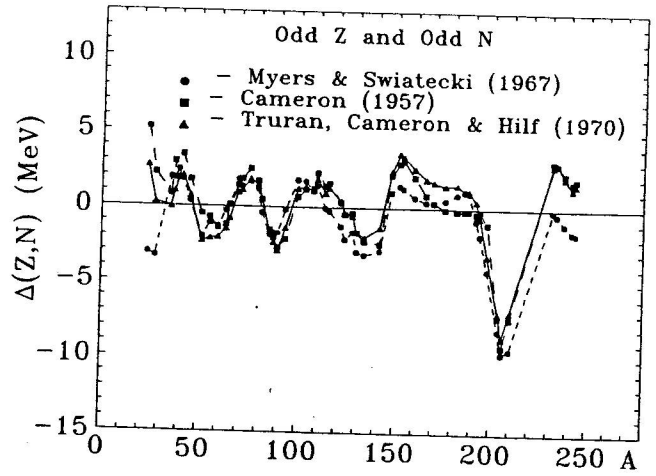

Fig. 1. Comparison of Cameron's [18], Truran, Cameron and Hilf's [19] and Myers and Swiatecki's [7] shell corrections.

with $\delta_f = 1.248$ MeV was suggested for $\delta^{BG77}(A,Z)$ [20]. The use of the LDM results in the parametrization of Cohen and Swiatecki [21] was suggested for the macroscopic part of the fission barriers $B_f^0(Z^2/A)$,

$$B_f^0(Z^2/A) = B_f^{LDM(CS63)} = \\ = a_S A^{2/3} \begin{cases} 0.83(1-x)^3, & \text{for } 2/3 < x < 1\,; \\ 0.38(3/4-x), & \text{for } 1/3 < x < 2/3\,, \end{cases} \quad (10)$$

where the fissility parameter x is given by

$$x = \frac{E_C^0}{2E_S^0} = \frac{Z^2/A}{(a_C/2a_S)\{1-k[(N-Z)/A]^2\}}, \quad (11)$$

$$a_S = 17.9439 \text{ MeV}, \quad a_C = 0.7053 \text{ MeV}, \quad k = 1.7826\,, \quad (12)$$

(LDM parameters from [7]), and the surface E_S^0 and Coulomb E_C^0 energies of a spherical nucleus are

$$E_S^0 = a_S\{1-k[(N-Z)/A]^2\}A^{2/3}, \quad (13)$$

$$E_C^0 = a_C Z^2/A^{1/3}. \quad (14)$$

The phenomenological representation (10) approximates very well the macroscopic LDM fission barriers (see Fig. 2) and provides satisfactory agreement of B_f^{BG77} with the experimental data and, as B_f^{BG77} are easily computed, it may be successfully used in Monte Carlo simulations of nuclear reactions involving fission.

LDM approaches

In the LDM, the experimental ground state mass for a nuclear equilibrium deformation α^0 is given by

$$M_{exp} = M_{LDM}^0(\alpha^0) + S^0(N,Z) + P^0(N,Z), \quad (15)$$

where M_{LDM}^0 is the LDM macroscopic mass, $S^0(N,Z)$ and $P^0(N,Z)$ are the shell and the pairing corrections, respectively. We have

$$M^f = M_{LDM}^f(\alpha^f) + S^f(N,Z) + P^f(N,Z) \quad (16)$$

for a fissioning nucleus (α^f is the saddle-point deformation). Substituting (15,16) into (1), we get

$$B_f = [M_{LDM}^f(\alpha^f) - M_{LDM}^0(\alpha^0)] + \\ + [S^f(N,Z) - S^0(N,Z)] + [P^f(N,Z) - P^0(N,Z)]. \quad (17)$$

Commonly, the last equation is written in the following form in the literature [1]:

$$B_f = B_f^0 - \delta W_{gs} + \delta W_{sp}, \quad (18)$$

where B_f^0 is the macroscopic LDM fission barrier, $\delta W_{gs} = S^0(N,Z)$ is the ground state shell correction and $\delta W_{sp} = S^f(N,Z) + P^f(N,Z) - P^0(N,Z)$ is the shell and pairing (or more exactly, the increase in the pairing energy between the transition state and ground state) correction at the saddle-point. Usually (see, e.g., [1]), one makes the assumption that the major shell structure effects vanish for a nucleus undergoing fission, as the nucleus deforms from the equilibrium ground state shape towards to the saddle-point one, i.e., $S^f(N,Z) = 0$. In general, there is no common point of view in literature, what is to be used for δW_{sp} in (18). So, some authors (e.g. [1, 22]) neglect this term; others (e.g., [16, 17, 20]) use different phenomenological approximations, and, finally, the third group (e.g., [23]) fits this term from the best description of experimental data.

In the notation of Nix [27], the potential energy of a deformed charged drop relative to the spherical drop (the macroscopic LDM fission barrier B_f^0) is

$$B_f^0 = E_S - E_S^0 + E_C - E_C^0 = \\ = [(B_S - 1) + 2x(B_C - 1)]E_S^0 \equiv b(x)E_S^0. \quad (19)$$

Here E_C^0 and E_C are the Coulomb energies of a spherical and a deformed drop, respectively; E_S^0 and E_S are their total surface energies; x is the fissility parameter

[1] In the present work, we confine ourselves to the analysis of single-humped fission barriers only. In the case of transuranium nuclides, the heights of double-humped fission barriers B_f^A and B_f^B are expressed by $B_f^i = \tilde{V}(\alpha_i) - \delta W_{gs} + \delta W_{sp}^i$, where $\tilde{V}(\alpha_i)$ is the macroscopic fission barrier and δW_{sp}^i is the shell correction for the i-th maximum of the potential energy, which is calculated from the liquid drop potential energy at corresponding deformation $\alpha_A \approx 0.3$ and $\alpha_B \approx 0.6$, $\delta W_{sp}^A \sim 2.80$ MeV, and $\delta W_{sp}^B \sim 0.50$ MeV [24]; and δW_{gs} is calculated in the LDM [7]. (For a more detailed information about double-humped fission barriers, see [23]-[26].)

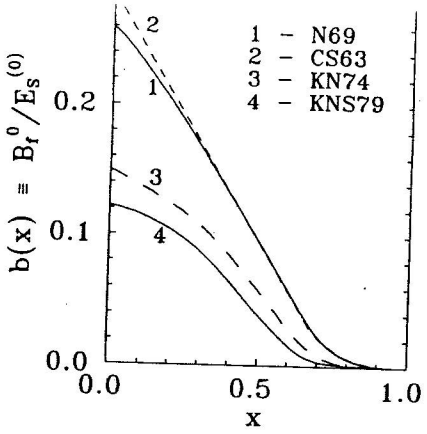

Fig. 2. Macroscopic fission barriers (units of E_S^0) as functions of the fissility parameter x for the LDM parameters [7] from [27] (marked as N69); in accordance with Cohen and Swiatecki's [21] parametrization (10) (CS63); for the single-Yukawa modified LDM of Krappe and Nix [13] (KN74); and for the Yukawa-plus-exponential modified LDM [14] (KNS79).

defined by (11); B_S and B_C are the relative surface and Coulomb energies depending on the deformation of the drop. They are tabulated (together with $b(x)$) in [27] as functions of the fissility parameter x; E_S^0 and E_C^0 are defined by (13) and (14). The values of constants a_S, a_C, and k obtained from the best existing LDM fit to nuclear masses and fission barriers [7] are given by (12). In other models, the values of these constants differ from (12), which also results in changing $b(x)$ and B_f^0. Fig. 2 shows the function $b(x)$ calculated with Myers and Swiatecki's parameters (12), in the framework of the single-Yukawa modified LDM [13] with

$$a_S = 24.7 \text{ MeV}, \quad a_C = 0.7448 \text{ MeV}, \quad k = 4.0 , \tag{20}$$

(nuclear radius parameter $r_0 = 1.16$ MeV and the range of the Yukawa function $a = 1.4$ fm), and in the framework of the Yukawa-plus-exponential modified LDM [14] with parameters

$$a_S = 21.7 \text{ MeV}, \quad a_C = 0.7322 \text{ MeV}, \quad a = 0.65 \text{ fm}, \quad r_0 = 1.18 \text{ fm}, \quad k = 2.04 ; \tag{21}$$

with the $b(x)$ parametrized by (10) in accord with Cohen and Swiatecki [21]. One can see that for medium and heavy nuclei the old approximation of Cohen and Swiatecki (10) agrees very well with the LDM [7] prediction for $b(x)$, and, being easily computed, it may be successfully used in numerical calculations.

For nuclei along Green's approximation to the line of β-stability [28]

$$N - Z = 0.4A^2/(A + 200) . \tag{22}$$

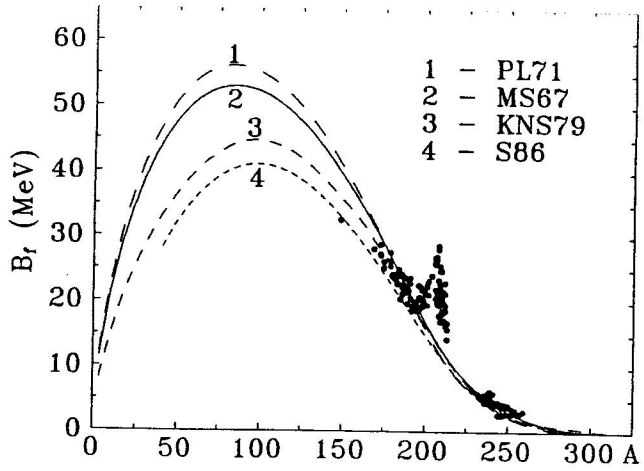

Fig. 3. Comparison of macroscopic fission barriers calculated for nuclei along Green's approximation to the line of β-stability in the LDM with Myers and Swiatecki's parameters [7] (marked as MS67); with Pauli and Ledergerber's LDM parameters [8] (PL71); in the Yukawa-plus-exponential modified LDM [14] (KNS79), and obtained with Sierk's subroutine BARFIT [15] (marked as S86). The experimental points are from [11, 29].

In Fig. 3, we compare macroscopic fission barriers calculated in the LDM with Myers and Swiatecki's parameters [7] (marked as MS67), in the Yukawa-plus-exponential modified LDM [14] (KNS79), and in the LDM with parameters of Pauli and Ledergerber [8] (PL71)

$$a_S = 19.008 \text{ MeV}, \quad a_C = 0.720 \text{ MeV}, \quad k = 2.84 . \tag{23}$$

For comparison, this Figure also shows the experimental data from Refs. [11, 29] and the results (marked as S86) obtained (for $L = 0$) with the subroutine BARFIT of Sierk [15], which provides fission barrier heights as functions of Z, A, and L by a multiparameter approximation of results obtained by the Yukawa-plus-exponential modified LDM with the following parameters

$$a_S = 21.13 \text{ MeV}, \quad a_C = 0.7448 \text{ MeV}, \quad a = 0.68 \text{ fm}, \quad r_0 = 1.16 \text{ fm}, \quad k = 2.3 . \tag{24}$$

One can see that fission barriers calculated for medium nuclei using Pauli and Ledergerber's parameters (23) are the highest ones ($B_f^{0(max)}(PL71) = 55.13$ MeV) and those calculated in the LDM [7] are the second highest ones ($B_f^{0(max)}(MS67) = 52.99$ MeV). Those calculated within the Yukawa-plus-exponential and single-Yukawa (KN74, see curve 2 in the low-right part of Fig.5) models are lying somewhat lower [$B_f^{0(max)}(KNS79) = 52.99$ MeV, $B_f^{0(max)}(S86) = 41.03$ MeV, and $B_f^{0(max)}(KN74) = 43.03$ MeV]. Three models, which include the finite range of nuclear force and the diffuse nuclear surface (KN74, KNS79, S86), yield results

that are very close together, although for all nuclei the barriers calculated with the Yukawa-plus-exponential model [14] they are slightly higher than those calculated within the single-Yukawa model [13]; the global approximation of Sierk [15] provides the lowest barrier heights.

In the present paper, we test seven models to calculate macroscopic fission barriers, namely, BITG73 [16], BG77 [17], MS67 [7], PL71 [8], KNS79 [14], KN74 [13], and S86 [15]. We test three sets of values of δW_{gs}, namely, the Cameron corrections $\Delta(Z,N)$ defined by eqs. (5) and (6), and the LDM shell corrections with Myers and Swiatecki's [7] parameters. For δW_{sp}, we test two sets of values, as defined by eqs. (7) and (9).

In Table 1, fission barriers calculated by phenomenological [16] and semi-phenomenological [17] methods with Cameron's [18] and Truran, Cameron and Hilf's [19] shell and pairing corrections are compared with the experimental values from the summary Table IV of Ref. [11].

Table 1

Calculated (in the framework of Refs. [16, 17]; with shell and pairing corrections from [18] and [19]) and experimental (Table IV of Ref. [11]) values of fission barriers

Isotope	Exp. [11]	Present calculations by different methods			
		BITG73[16] shell & pair. corr. [18]	BITG73[16] shell & pair. corr. [19]	BG77[17] shell & pair. corr. [18]	BG77[17] shell & pair. corr. [19]
$^{173}Lu_{71}$	27.3	27.65	25.62	32.40	30.36
$^{179}Ta_{73}$	26.2	24.04	29.93	27.72	25.49
$^{188}Os_{76}$	23.7	22.62	25.22	23.77	21.25
$^{187}Os_{76}$	22.5	22.36	25.24	23.82	20.86
$^{186}Os_{76}$	22.5	21.59	24.49	22.85	20.54
$^{191}Ir_{77}$	22.8	21.74	24.14	23.01	21.19
$^{189}Ir_{77}$	21.7	20.49	23.49	21.92	19.78
$^{198}Hg_{80}$	21.8	22.11	19.72	21.40	20.61
$^{201}Tl_{81}$	22.3	22.47	21.12	22.60	21.27
$^{209}Bi_{83}$	22.6	24.24	24.68	24.10	23.66
$^{207}Bi_{83}$	21.2	21.91	22.75	22.77	21.69
$^{212}Po_{84}$	18.6	19.62	19.44	19.24	20.05
$^{211}Po_{84}$	21.5	20.21	20.91	20.80	20.74
$^{210}Po_{84}$	20.4	19.93	21.47	21.21	21.48
$^{213}At_{85}$	16.8	15.32	17.45	17.39	18.00
$^{227}Ra_{88}$	8.30	8.22	8.91	8.53	8.22
$^{233}Th_{90}$	6.44	7.35	7.48	7.30	7.55
$^{232}Th_{90}$	5.95	6.65	6.71	6.46	7.33
$^{232}Pa_{91}$	6.18	6.09	6.77	6.95	6.45
$^{239}U_{92}$	6.29	6.71	6.32	6.24	7.01
$^{238}U_{92}$	5.60	6.13	5.63	5.51	6.86
$^{237}U_{92}$	6.40	6.56	6.32	6.28	6.69
$^{236}U_{92}$	5.44	6.00	5.54	5.57	6.50

Table 1 (*continued*)

Isotope	Exp. [11]	Present calculations by different methods			
		BITG73[16] shell & pair. corr. [18]	BITG73[16] shell & pair. corr. [19]	BG77[17] shell & pair. corr. [18]	BG77[17] shell & pair. corr. [19]
$^{235}U_{92}$	5.75	6.32	6.05	6.23	6.31
$^{234}U_{92}$	5.30	5.66	5.28	5.40	6.09
$^{233}U_{92}$	5.49	6.05	5.72	6.11	5.87
$^{238}Np_{93}$	6.04	6.01	6.24	6.46	6.15
$^{237}Np_{93}$	5.49	5.46	5.47	5.75	5.97
$^{244}Pu_{94}$	4.60	5.76	4.73	4.75	6.32
$^{242}Pu_{94}$	4.70	5.48	4.57	4.67	6.10
$^{241}Pu_{94}$	6.20	5.93	5.26	5.45	5.97
$^{240}Pu_{94}$	4.85	5.38	4.58	4.73	5.83
$^{239}Pu_{94}$	5.48	5.83	5.28	5.52	5.67
$^{238}Pu_{94}$	4.70	5.29	4.51	4.82	5.49
$^{236}Pu_{94}$	4.55	5.00	4.28	4.68	5.10
$^{244}Am_{95}$	6.21	5.70	5.48	5.81	5.77
$^{242}Am_{95}$	6.40	5.60	5.47	5.88	5.53
$^{241}Am_{95}$	6.00	5.05	4.80	5.17	5.38
$^{250}Cm_{96}$	4.10	5.35	3.66	4.04	5.69
$^{248}Cm_{96}$	4.25	5.56	4.22	4.44	5.60
$^{246}Cm_{96}$	4.35	5.37	4.08	4.44	5.45
$^{244}Cm_{96}$	4.25	5.13	3.94	4.38	5.25
$^{242}Cm_{96}$	4.25	5.06	3.97	4.47	4.99
$^{240}Cm_{96}$	4.15	5.00	3.92	4.57	4.68
$^{250}Bk_{97}$	5.80	5.51	4.90	5.37	5.27
$^{249}Bk_{97}$	4.35	5.15	4.52	4.85	5.22
$^{252}Cf_{98}$	3.65	4.94	3.26	3.81	4.95
$^{250}Cf_{98}$	3.95	5.18	3.84	4.23	4.88
$^{248}Cf_{98}$	3.85	5.01	3.72	4.25	4.75
$^{246}Cf_{98}$	3.85	4.80	3.60	4.21	4.57
$^{254}Fm_{100}$	3.35	4.50	3.00	3.66	4.36
$^{248}Fm_{100}$	2.75	4.40	3.41	4.13	4.04
$^{246}Fm_{100}$	2.55	4.36	3.50	4.28	3.83
$^{245}Fm_{100}$	2.62	4.84	4.23	5.10	3.71
$^{244}Fm_{100}$	2.62	4.33	3.50	4.44	3.57

One can see that both these methods give results quite consistent with experimental data, although the approach proposed in [16] predicts fission barriers slightly closer to the experimental data for lighter nuclei and worse for heavier ones, independently of what shell corrections from [18, 19] we use. The results obtained with different shell corrections from [18, 19] differ appreciably only for neutron-rich and neutron-deficient nuclei. In these cases, the use of shell corrections from [19] seems to be more preferable.

The results of calculations of macroscopic fission barriers according to models [7, 8, 13–15] with Myers and Swiatecki's [7] shell corrections for microscopic parts of barriers are compared in Table 2 to the same experimental data. One can see that all these methods provide fission barriers quite close to the experimental data.

Table 2

Calculated (macroscopic B_f^0 – in accordance with [7, 8, 13–15] and shell corrections from [7]) and experimental (Table IV of Ref. [11]) values of fission barriers.

Isotope	Exp. [11]	Present calculations by different methods					
		MS67 [7]	PL71 [8]	KN74 [13]	KNS79 [14]	S86[15] without shell cor.	S86[15] with shell cor. [7]
$^{173}Lu_{71}$	27.3	28.28	28.93	24.85	27.01	24.13	23.69
$^{179}Ta_{73}$	26.2	25.49	25.73	22.44	24.69	22.12	21.43
$^{188}Os_{76}$	23.7	21.25	20.89	18.77	20.31	19.03	18.06*
$^{187}Os_{76}$	22.5	20.86	20.81	18.96	20.27	18.84	17.78
$^{186}Os_{76}$	22.5	20.54	20.79	19.21	20.30	18.65	17.57
$^{191}Ir_{77}$	22.8	21.19	20.65	18.93	20.45	17.98	18.31
$^{189}Ir_{77}$	21.7	19.78	19.84	18.65	19.72	17.63	17.11
$^{198}Hg_{80}$	21.8	20.61	20.17	19.99	20.85	14.60	18.81
$^{201}Tl_{81}$	22.3	21.27	20.71	20.74	21.55	13.61	19.71
$^{209}Bi_{83}$	22.6	23.66	22.44	22.04	23.37	11.94	22.30
$^{207}Bi_{83}$	21.2	21.69	20.94	21.03	21.94	11.70	20.49
$^{212}Po_{84}$	18.6	20.05	18.78	18.45	19.72	11.00	18.82
$^{211}Po_{84}$	21.5	20.74	19.70	19.60	20.68	10.90	19.60
$^{210}Po_{84}$	20.4	21.48	20.65	20.77	21.67	10.79	20.40
$^{213}At_{85}$	16.8	18.00	17.13	17.27	18.13	9.90	17.02
$^{227}Ra_{88}$	8.30	8.22	6.39	5.46	7.09	7.81	7.10
$^{233}Th_{90}$	6.44	7.55	5.82	5.00	6.39	6.34	6.51
$^{232}Th_{90}$	5.95	7.33	5.76	5.06	6.36	6.30	6.34
$^{232}Pa_{91}$	6.18	6.45	5.34	5.09	5.95	5.49	5.63
$^{239}U_{92}$	6.29	7.01	5.41	4.80	5.84	5.06	6.04
$^{238}U_{92}$	5.60	6.86	5.39	4.87	5.84	5.03	5.93
$^{237}U_{92}$	6.40	6.69	5.35	4.94	5.83	4.99	5.80
$^{236}U_{92}$	5.44	6.50	5.29	4.99	5.80	4.94	5.66
$^{235}U_{92}$	5.75	6.31	5.22	5.02	5.75	4.89	5.50
$^{234}U_{92}$	5.30	6.09	5.13	5.05	5.69	4.84	5.33
$^{233}U_{92}$	5.49	5.87	5.02	5.06	5.60	4.78	5.14
$^{238}Np_{93}$	6.04	6.15	5.09	4.95	5.56	4.34	5.37
$^{237}Np_{93}$	5.49	5.97	5.02	4.99	5.52	4.29	5.23
$^{244}Pu_{94}$	4.60	6.32	4.97	4.62	5.39	3.95	5.46
$^{242}Pu_{94}$	4.70	6.10	4.97	4.79	5.42	3.88	5.32

Table 2 (*continued*)

Isotope	Exp. [11]	Present calculations by different methods					
		MS67 [7]	PL71 [8]	KN74 [13]	KNS79 [14]	S86[15] without shell cor.	S86[15] with shell cor. [7]
$^{241}Pu_{94}$	6.20	5.97	4.94	4.86	5.41	3.84	5.22
$^{240}Pu_{94}$	4.85	5.83	4.90	4.91	5.38	3.79	5.11
$^{239}Pu_{94}$	5.48	5.67	4.84	4.95	5.34	3.75	4.97
$^{238}Pu_{94}$	4.70	5.49	4.77	4.97	5.28	3.70	4.83
$^{236}Pu_{94}$	4.55	5.10	4.57	4.97	5.11	3.58	4.48
$^{244}Am_{95}$	6.21	5.77	4.77	4.74	5.25	3.38	5.05
$^{242}Am_{95}$	6.40	5.53	4.72	4.86	5.23	3.30	4.86
$^{241}Am_{95}$	6.00	5.38	4.68	4.90	5.20	3.25	4.75
$^{250}Cm_{96}$	4.10	5.69	4.46	4.36	4.87	3.05	4.91
$^{248}Cm_{96}$	4.25	5.60	4.55	4.56	5.00	2.99	4.89
$^{246}Cm_{96}$	4.35	5.45	4.58	4.70	5.07	2.93	4.80
$^{244}Cm_{96}$	4.25	5.25	4.56	4.82	5.07	2.85	4.65
$^{242}Cm_{96}$	4.25	4.99	4.47	4.88	5.01	2.75	4.43
$^{240}Cm_{96}$	4.15	4.68	4.31	4.89	4.88	2.65	4.15
$^{250}Bk_{97}$	5.80	5.27	4.36	4.53	4.76	2.58	4.63
$^{249}Bk_{97}$	4.35	5.22	4.39	4.62	4.81	2.55	4.61
$^{252}Cf_{98}$	3.65	4.95	4.16	4.49	4.54	2.22	4.38
$^{250}Cf_{98}$	3.95	4.88	4.23	4.66	4.64	2.16	4.35
$^{248}Cf_{98}$	3.85	4.75	4.24	4.78	4.68	2.08	4.26
$^{246}Cf_{98}$	3.85	4.57	4.20	4.84	4.66	2.00	4.11
$^{254}Fm_{100}$	3.35	4.36	3.89	4.56	4.26	1.55	3.96
$^{248}Fm_{100}$	2.75	4.04	3.89	4.84	4.31	1.33	3.71
$^{246}Fm_{100}$	2.55	3.83	3.77	4.82	4.21	1.25	3.51
$^{245}Fm_{100}$	2.62	3.71	3.69	4.79	4.13	1.21	3.39
$^{244}Fm_{100}$	2.62	3.57	3.59	4.74	4.04	1.16	3.25

Figs. 4 and 5 show fission barriers calculated using methods of Refs. [7, 8, 13, 14, 16, 17] for nuclei along the line of β-stability together with the experimental data. As one can see, all the methods provide fission barriers in good agreement with experimental data for heavy nuclei. Here, the semi-phenomenological approach of Barashenkov and Gereghi [17] permanently overestimates the experimental data for nuclei lighter than Pb. Apparently, the Yukawa-plus-exponential modified LDM [14] provides the best agreement of calculated barriers to the experimental data of nuclei along the line of β-stability.

Excitation energy dependence of fission barriers

The change of properties of atomic nuclei with increasing excitation energies influences strongly the nuclear fissility. The calculations by the Thomas-Fermi [32] and the Hartree-Fock [31] methods predict that "thermal" effects must lead to the

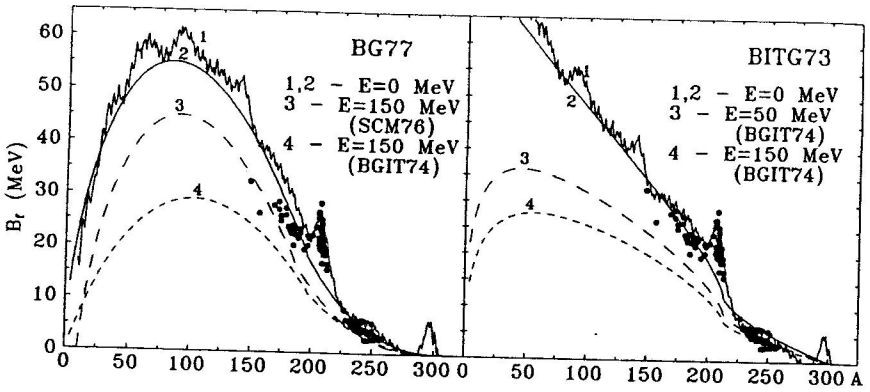

Fig. 4. Comparison of fission barriers predicted by phenomenological [16] (BITG73) and semiphenomenological [17] (BG77) approaches with the experimental data [11, 29] for nuclei along the line of β-stability. The solid lines are the results for zero excitation energy (smooth lines — only the macroscopic part of B_f; "irregular" lines — Cameron's [18] shell and pairing corrections). The dashed lines show the results of calculations for excited nuclei; the values of excitation energies E are indicated in the Figure. The results of calculations for the dependence of fission barriers on the excitation energy as proposed in [30] are marked as BGIT74; SCM76 denotes those proposed in [31].

decrease of B_f. The investigations of the dependence of B_f on nuclear temperature T [31]-[34] show that the dependences of Coulomb E_C^0 and surface E_S^0 energies on T are

$$\begin{aligned} E_S(T) &= E_S(0)[1-\beta T^2] \\ E_C(T) &= E_C(0)[1-\alpha T^2], \end{aligned} \qquad (25)$$

where the nuclear temperature T is given by

$$T = \sqrt{E/a} \ ; \qquad E \equiv E^* - \Delta_f \ .$$

Here, E^* and a are the excitation energy and level density parameter of a nucleus, respectively; $\Delta_f = \chi \cdot 14/\sqrt{A}$ [MeV] is the pairing energy of a fissioning nuclei ($\chi = 0$, 1, and 2 for odd-odd, odd-even, and even-even nuclei, respectively). It was found that [31]

$$\alpha = 1 \cdot 10^{-3}\ \mathrm{MeV}^{-2}, \quad \beta = 6.3157 \cdot 10^{-3}\ \mathrm{MeV}^{-2} \ . \qquad (26)$$

Barashenkov *et al.* [30] proposed to estimate the dependence of B_f on E^* by the following empirical relation

$$B_f(E) = B_f(0)/(1+\sqrt{E/2A}) \qquad (27)$$

Earlier, Yamaguchi [35] has derived by the means of classical thermodynamics

$$B_f(E) = B_f(0)(1-E/E_0),$$

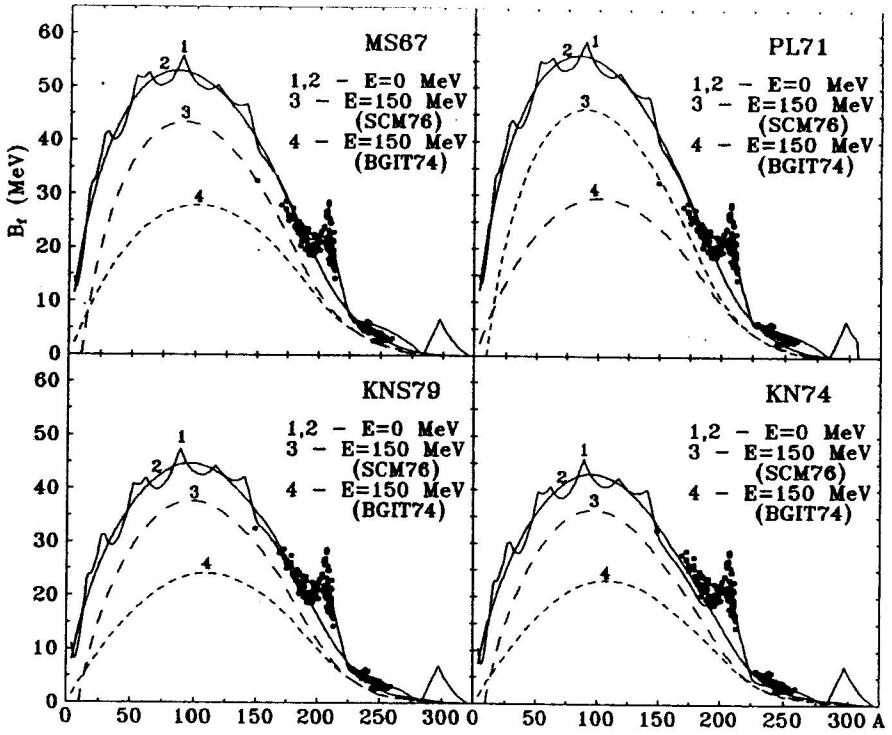

Fig. 5. Comparison of fission barriers calculated in the framework of the LDM [7] (MS67), the LDM [8] (PL71), the Yukawa-plus-exponential modified LDM [14] (KNS79), and the single-Yukawa modified LDM [13] (KN74) with the experimental data [11, 29] for nuclei along the line of β-stability. The remaining notation is the same as in Fig. 4.

where $E_0 = aT_0^2$, $T_0 \simeq 9$ MeV.

A recent attempt of Newton, Popescu and Leigh [36] interpolates the results of Garcias *et al.* [2] [37] on the evolution of the fission barriers as a function of temperature and angular momentum by a simple formula that can be incorporated in a statistical model code.

In the present paper, we estimate the influence of "thermal" effects on the fission barrier B_f (see Figs. 4 and 5) in two ways, namely, by using the relation (25) with α and β given by (26) for $a = A/10$ (the results are marked as SCM76), and by a phenomenological relation (27) (BGIT74). One can see that the phenomenological approach (27) provides faster decrease in B_f with increasing excitation energy in comparison with the approach (25). This is highly appreciable

[2] Recently, Garcias *et al.* [37] calculated nuclear fission barriers using Thomas-Fermi model with the Skyrme force, which self-consistently incorporates the effects of rotations and temperature. But this method is too complicated to be used commonly in Monte Carlo calculations of fission processes.

for medium weight and light nuclei with the energies of excitation above 50 MeV. "Thermal" effects may cause tenfold increase of the nuclear fissility for $Z^2/A \leq 27$ (see, for example, [38]).

Dependence of fission barrier heights on the rotation of nuclei

It has been found from the measured angular correlations and distributions of fission fragments produced in the bombardment of ^{232}Th targets with different projectiles that the upper limits of the mean angular momenta transferred to the fissioning nuclei are small [39] in the case of proton-induced reactions. As seen from Table 3, only a small fraction of the grazing angular momentum is left in the

Table 3

The mean angular momentum transfers $< L >$ of fissioning nuclei and the maximum possible angular momentum in the entrance channel (grazing angular momentum) l_{max} for different reactions [39]

System	E_i, MeV	l_{max}, $\hbar$	$< L >$, $\hbar$
p+^{232}Th	140	25	4
	250	35	1
	500	49	1
	1000	70	1
d+^{232}Th	70	25	13
	140	37	11
	500	72	5
	1000	102	5
α+^{232}Th	280	75	17
	1000	148	7
α+^{197}Au	280	72	28

fissioning nuclei. Large relative angular momenta in the entrance channels seem to be taken away by cascade ejectiles or by fast pre-equilibrium particles [39]. Therefore, it is possible to neglect the dependence of B_f on the angular momenta L of fissioning nuclei in calculations of such reactions in the first order. On the contrary, the momenta of fissioning nuclei are high in heavy-ion induced reactions (see, e.g., [4]), and the dependence of B_f on L must be taken into account.

Several approaches are presently used for the description of fission barrier dependence on angular momenta of rotating nuclei. One of the most extensively used and perhaps the most successful theoretical model for this purpose is the Rotation-Liquid-Drop Model (RLDM) of Cohen, Plasil and Swiatecki [9]. However, questions have been raised about the general validity of the RLDM [40, 41].

Mustafa *et al.* [10] have proposed a model which differs from the RLDM in the shape parametrization and in the calculation of the Coulomb, surface, and rotation energies. The authors of [10] used the two-center-model shape parametrization

which allows for triaxial shape variations and a continuous transition from one-center to two-center shapes with a smooth neck. They calculated the surface energy with the Yukawa-plus-exponential folding function of Krappe, Nix and Sierk [14], which incorporates the effects of the finite range of nuclear force and of the diffuse nuclear surface, and calculated both the Coulomb and rotation energies with surface diffuseness described by the Yukawa folding function.

A further development of this approach has been done by Sierk [15]. He used highly accurate numerical techniques, flexible shape parametrization which allows accurate estimation of the convergence of results as a function of the number of degrees of freedom of the nuclear shapes considered, and a better set of parameters for calculations in comparison with [10]. In addition, Sierk approximated his results for hundreds of nuclei in a usable form in two computer subroutines BARFIT and MOMFIT, which provide accurate values for fission barrier heights and saddle-point moments of inertia as the functions of Z, A and L. These subroutines can be easily incorporated in statistical evaporation models.

At last, one has to mention phenomenological approach frequently used in statistical calculations (e.g. [16, 42]) to estimate the dependence of B_f on L, wherein one assumes that the nuclear rotation energy E_R is not available for excitation energy released in the fission and evaporation processes. This implies that the fission barrier $B_f(L)$ of a fissioning nucleus with the angular momentum L can be written as

$$B_f(L) = B_f(0) - (E_R^{gs} - E_R^{sp}). \tag{28}$$

Here, E_R^{gs} and E_R^{sp} are nuclear rotational energies for the ground state and at the saddle-point, respectively,

$$E_R^{gs} = \frac{L(L+1)\hbar^2}{2\mathcal{J}_{rb}},$$

$$E_R^{sp} = \frac{L(L+1)\hbar^2}{2\mathcal{J}_{sp}}, \tag{29}$$

$$\mathcal{J}_{rb} = 0.4 M_n r_0^2 A^{5/3}. \tag{30}$$

L is the angular momentum of nucleus, M_n is the nucleon mass, and the values calculated and plotted in [43] or tabulated in [21] are used for the moment of inertia of a nucleus at the saddle-point $\mathcal{J}_{sp}$.

As seen from Fig. 6, Strutinsky's [43] results for moments of inertia of nuclei at the saddle-point are very close to the Cohen and Swiatecki ones [21]; thus, concrete numerical calculations may be done with any one of them.

As an example, Fig. 7 shows macroscopic fission barriers of rotating nuclei with different values of angular momentum L calculated in accordance with eqs. (28-30) with the LDM parameters [7], and Strutinsky's values for $\mathcal{J}_{sp}$ [43], and, for a comparison, also fission barriers computed with Sierk's subroutine BARFIT as functions of the mass number for β-stable nuclei. One can see that phenomenological approach (28-30) with LDM [7] predicts significantly higher values for fission barriers than the Yukawa-plus-exponential model [15] for small values of the angular momentum L and $A \leq 200$. However, the results obtained in both these

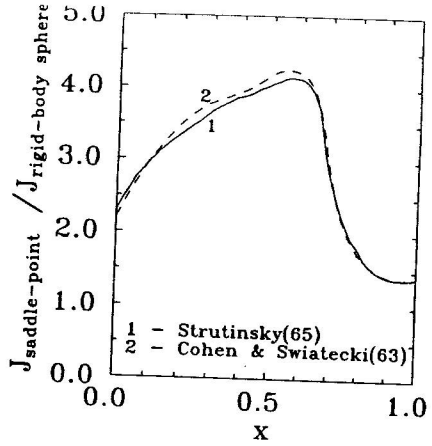

Fig. 6. Comparison of Strutinsky's [43] and Cohen and Swiatecki's [21] prediction of moments of inertia of nuclei at the saddle-point as functions of the fissility parameter x.

approaches are similar for $A > 200$ and/or high values of the nuclear angular momentum L.

Fig. 8 shows the fission barrier heights calculated within different models as functions of the angular momentum L for ^{153}Tb, ^{176}Os, and ^{229}Np. One can see that the barriers calculated phenomenologically according to (28-30) in the LDM [7] are similar to those calculated in the Yukawa-plus-exponential model [5] and to Mustafa's *et al.* [10] predictions. Our calculations show that Sierk's subroutine BARFIT [15] needs about a tenfold increase of computing time in comparison with these phenomenological calculations. Thus, we can successfully use the phenomenological approach (28-30) to estimate the dependence of fission barriers on the angular momentum of nucleus in real Monte Carlo calculations which need much computing time to obtain a good statistics.

III. ANALYSIS OF FISSILITY OF EXCITED COMPOUND NUCLEI

Basic relations for particle emission and fission widths

In this section, we will use the fission barriers considered above to analyze the energy dependence of the fissility of different excited compound nuclei. In the Weisskopf statistical theory of particle emission [44] and the Bohr and Wheeler [45] theory of fission, the partial widths Γ_j for the emission of a particle j ($j \equiv n, p, d, t, ^3$He, α) and Γ_f for fission are expressed by the approximate formulae (units: $\hbar = c = 1$; see, e.g., [23, 42]):

$$\Gamma_j = \frac{(2s_j+1)m_j}{\pi^2\rho_c(U_c)} \int_{V_j}^{U_j-B_j} \sigma_{inv}^j(E)\rho_j(U_j - B_j - E)E\mathrm{d}E\,, \qquad (31)$$

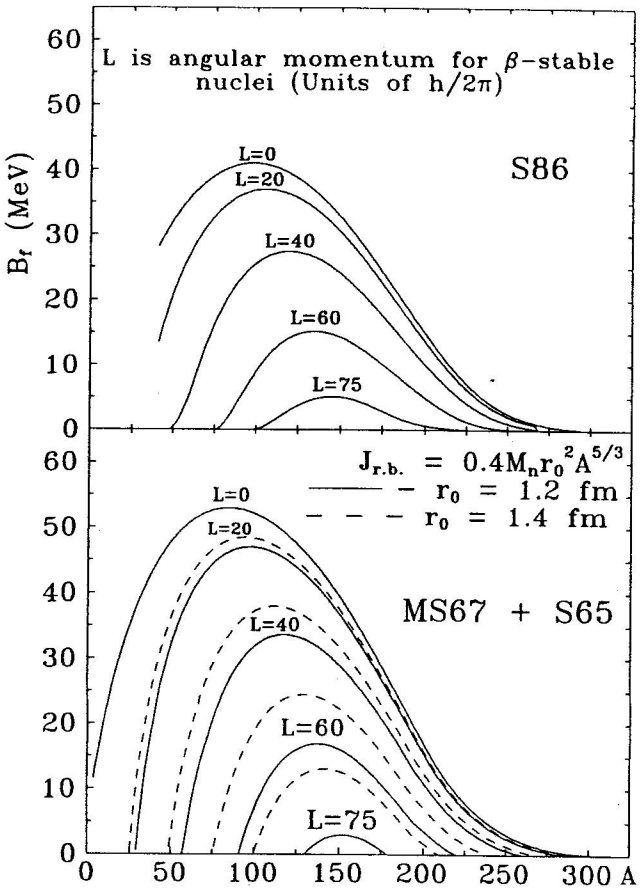

Fig. 7. Calculated fission barriers of rotating nuclei with different values of the nuclear angular momentum L as functions of the mass number for β-stable nuclei. Lower Fig.: the LDM [7] with Strutinsky's [43] values for moments of inertia of nuclei at the saddle-point, in accordance with (28-30); upper Fig.: predictions of Sierk's [15] subroutine BARFIT.

$$\Gamma_f = \frac{1}{2\pi\rho_c(U_c)} \int_0^{U_f-B_f} \rho_f(U_f - B_f - E)\mathrm{d}E\,. \qquad (32)$$

Here, ρ_c, ρ_j, and ρ_f are the level densities of the compound nucleus, the residual nucleus produced after the emission of the j-th particle, and of the fissioning nucleus at the fission saddle point, respectively; m_j, s_j and B_j are the mass, spin and the binding energy of the j-th particle, respectively; B_f is the fission barrier height. We calculate the binding energies of particles using the Cameron formulae [18];

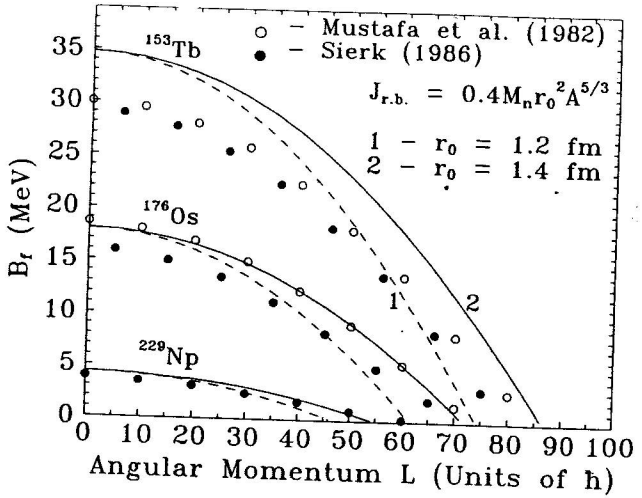

Fig. 8. Calculated fission barriers as functions of the angular momentum for ^{153}Tb, ^{176}Os and ^{229}Np. Solid and dashed lines are our calculations in accord with (28-30) for the LDM [7] and Strutinsky's [43] values for moments of inertia of nuclei at the saddle-point for r_0 = 1,4 fm and r_0 = 1.2 fm, respectively. The open circles show the tabulated results of Mustafa *et al.* [10]. The solid circles are the results obtained with the subroutine BARFIT of Sierk [15].

$\sigma^j_{inv}(E)$ is the inverse cross-section for absorption of the j-th particle with kinetic energy E by the residual nucleus. The approximation proposed by Dostrovsky [46] is used,

$$\sigma^j_{inv}(E) = \sigma^j_{geom}\alpha_j\left(1+\frac{\beta_j}{E}\right) , \qquad (33)$$

where

$$\sigma^j_{geom} = \pi R_j^2 \; ; \quad R_j = \tilde{r}_0 A_{fj}^{1/3} \; ; \quad \tilde{r}_0 = 1.5 \text{ fm} \; ;$$
$$\alpha_n = 0.76 + 2.2A_{fj}^{-1/3} \; ; \quad \beta_n = (2.12A_{fj}^{-2/3} - 0.05)/\alpha_n \; .$$

For charged particles $\beta_j = -V_j$, where V_j is the effective Coulomb barrier and the constants α_j are calculated for given nucleus by interpolation of the values of Ref. [46]. The angular momentum dependence of the level density is done by $\rho(E^*, L) = \rho(U, 0)$ where $U = E^* - E_R$ and E_R are the "thermal" and rotational energies of the nucleus, respectively;

$$U_c = E^* - E^c_R - \Delta_c \; ; \quad U_j = E^* - E^j_R - \Delta_j \; ; \quad U_f = E^* - E^f_R - \Delta_f \; .$$

Here, E^* is the total excitation energy of the compound nucleus; E^c_R, E^j_R, and E^f_R are the rotational energies for the compound, residual, and fissioning nucleus at the saddle point, respectively, and they are determined by (29,30);

$$\Delta_c = \chi \cdot 12\sqrt{A_c} \; ; \quad \Delta_j = \chi \cdot 12\sqrt{A_{fj}} \; ; \text{ and } \Delta_f = \chi \cdot 14\sqrt{A_c} \text{ (MeV)}$$

are the pairing energies of the compound and residual nuclei, and of the fission saddle point, respectively; $A_{fj} = A_c - A_j$, where A_c and A_j are the mass numbers of the compound nucleus and of the j-th particle, respectively.

Particle emission and fission widths (31–32) are obtained within the Fermi-gas approach to the nuclear level density

$$\rho(E^*) = const \cdot \exp\{2\sqrt{aE^*}\} \; .$$

Thus (see, e.g., [47])

$$\Gamma_j = \frac{(2s_j+1)m_j\alpha_j\tilde{r}_0^2A_{fj}^{2/3}}{\pi a_j \exp(2\sqrt{a_cU_c})}\{(U_j - B'_j)[1+(k_j-1)\exp(k_j)] - \\ - [6+(k_j^3 - 3k_j^2 + 6k_j - 6)\exp(k_j)]/(4a_j)\} \; , \qquad (34)$$

$$\Gamma_f = \frac{1+(k_f-1)\exp(k_f)}{4\pi a_f \exp(2\sqrt{a_cU_c})} \; , \qquad (35)$$

where $B'_n = B_n - \beta_n$; $B'_{j\neq n} = B_j + V_j$; $k_j = 2\sqrt{a_j(U_j - B'_j)}$; $k_f = 2\sqrt{a_f(U_f - B_f)}$, and a_c, a_j, and a_f are the level density parameters of the compound and residual nuclei, and of the fission saddle point, respectively.

In the case of transuranium nuclei, when double-humped fission barriers are used, we define the fission width by the expression (see, e.g., [23]):

$$\Gamma_f = \frac{\Gamma_A\Gamma_B}{\Gamma_A + \Gamma_B} \; , \qquad (36)$$

where Γ_A and Γ_B are the partial widths for the corresponding saddle points. We calculate each of these widths by formula (35) with its own shell correction.

Comparison with Experiment

A lot of experimental data are now available on the nuclear fissility and fission cross-section of heavy nuclei induced by different probes (reviews [1]-[4]). The fissility is the ratio of the fission cross-section to the inelastic interaction cross-section $P_f = \sigma_f/\sigma_{in}$. For a given excited compound nucleus, the fissility may be estimated as the ratio of partial widths Γ_f/Γ_{tot}, where $\Gamma_{tot} = \Gamma_f + \sum_j \Gamma_j$.

We have analyzed practically all the data on nuclear fissility published in review [1] using formulae (34-35) and fission barriers regarded above. Let us show here only some of the results. As an example, measured [1] and calculated fissilities for ^{189}Ir, ^{188}Os, ^{189}Ta, and ^{173}Lu nuclides are shown in Fig. 9. The calculations were performed using fission barriers from Ref. [14] without taking into account the dependence of B_f on the excitation energy E^*, with Cameron's [19] shell and pairing corrections, the third Iljinov, Mebel's *et al.* systematics for the level density parameter without an explicit taking into account of collective effects, for the values of the ratio a_f/a_n indicated in the Figure. One can see that one obtains a good description of experimental data in this approach. Our analysis shows that

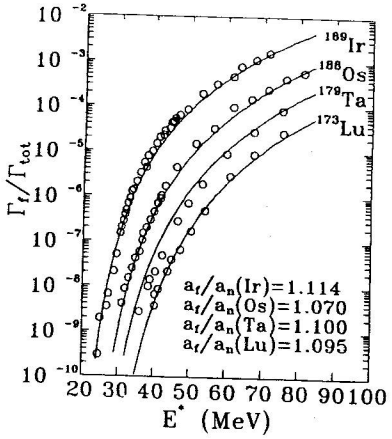

Fig. 9. Excitation energy dependence of the fissility Γ_f/Γ_{tot} of different nuclei. Curves are the results of our calculation with KNS79 [14] fission barriers, C70 [19] shell corrections, the third Iljinov, Mebel *et al.* [23] systematics for the level density parameter without the explicit taking into account of collective effects. Experimental points were taken from the review [1]. The used values for the ratio a_f/a_n are shown in Figure.

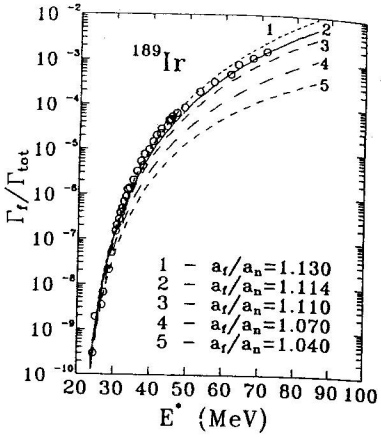

Fig. 10. Dependence of the calculated fissility of the excited ^{189}I compound nucleus on the values of a_f/a_n. The remaining notation is the same as in Fig. 9.

it is possible to select a concrete model for the fission barrier, shell and pairing corrections for every nuclide, a systematics for the level density parameter, and to fit the value of the ratio a_f/a_n to obtain very good description of the experimental data. But it is not possible to describe well the experimental fissilities for all nuclides with a fixed set of these options.

Calculated fissilities are the most sensitive to the used values of the ratio a_f/a_n. As an example, Fig. 10 shows how the calculated fissility of the excited ^{189}Ir nuclide depends on the ratio a_f/a_n. One can see that for high excitation energies $E^* > 50$ MeV a small increase of the ratio a_f/a_n from 1.04 to 1.13 results in an increase of the calculated fissility more than one order of magnitude.

Fig. 11 shows the fissilities of the ^{189}Ir nuclide for the ratio $a_f/a_n = 1.114$ obtained using the third Iljinov *et al.* systematics for the level density parameters [23], Cameron's [19] shell and pairing corrections calculated with different fission barriers, namely, BITG73 [16], BG77 [17], MS67 [7], PL71 [8], KN74 [13], KNS79 [14], and S86 [15] without taking into account the dependence of B_f on E^*. One can see that all fission barriers used provide a correct description of the shape of the calculated curves in this case, and by fitting the value of the ratio a_f/a_n it is

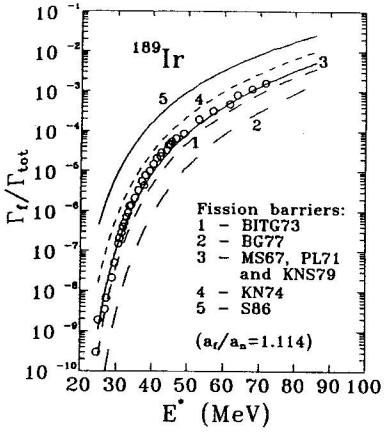

Fig. 11. Dependence of the fissility of the excited ^{189}I compound nucleus on the fission barriers used. Calculations done with MS67, PL71 and KNS79 fission barriers are indistinguishable in the scale of this picture. The other notation is the same as in Fig. 9.

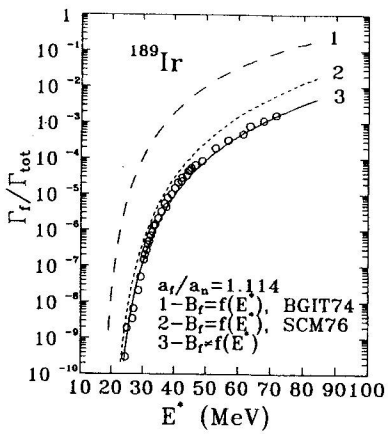

Fig. 12. Dependence of the fissility of the excited ^{189}I compound nucleus on the form of the excitation energy dependence of fission barriers $B_f(E^*)$. The remaining notation is the same as in Fig. 9. Dependence of the calculated fissility of the excited ^{189}I compound nucleus on the values of a_f/a_n. The remaining notation is the same as in Fig. 9.

possible to obtain a good description also for the absolute value of the fissility for each of the models for B_f.

An example of the dependence of the calculated fissilities on the form of the energy dependence of the fission barriers $B_f(E^*)$ is shown in Fig. 12. Our analysis shows that it is possible to fit the value of the ratio a_f/a_n and to describe the data with the dependences $B_f(E^*)$ proposed by Barashenkov *et al.* [30] and by Sauer *et al.* [31], as well as without explicit dependence of B_f on E^* within the interval of energies regarded here. To elucidate better this question, it is necessary to analyze the fissilities and fission cross-sections in a larger range of incident/excitation energies.

An example of influence of the angular momentum on the fissility of an excited fissioning nucleus is shown in Fig. 13. One can see that we can neglect the dependence of the fission barriers on the angular momentum in calculations of the nuclear fissilities for small values of the angular momentum $L < 20$ (that is, e.g., the case of nucleon-nucleus interactions at intermediate energies). On the contrary, taking into account the dependence $B_f(L)$ not only increases the absolute values of the fissilities several orders of magnitude for high values of L (e.g. in heavy-ion induced reactions), but it also significantly changes the shape of the dependence of nuclear fissility on the excitation energy of a rotating fissioning nucleus.

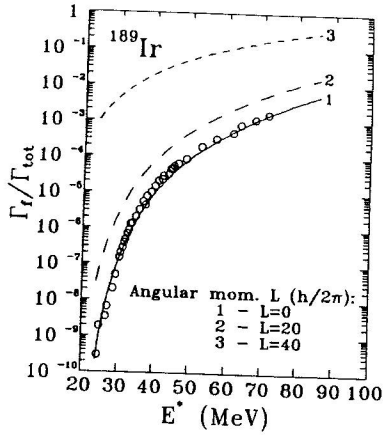

Fig. 13. Dependence of the fissility of the excited ^{189}I compound nucleus on the value of its angular momentum L. The dependence of fission barriers on the angular momentum $B_f(L)$ were calculated from the formulae (28-30) with $r_0 = 1.2$ fm. The remaining notation is the same as in Fig. 9.

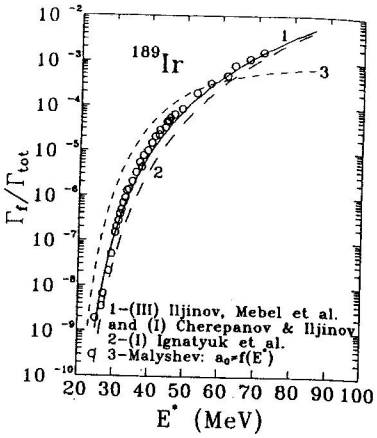

Fig. 14. Dependence of the fissility of the excited ^{189}I compound nucleus on the systematics for the level density parameter used in calculations; $a_f/a_n = 1.114$. Calculations using the first Cherepanov and Iljinov and the third Iljinov, Mebel's *et al.* systematics for $a(Z, N, E^*)$ are indistinguishable in the scale of this picture. The remaining notation is the same as in Fig. 9.

Fig. 14 shows how theoretical fissility depends on the systematics for the level density parameter used in the calculations. One can see that Malyshev's systematics for $a(Z, N)$ provides a good description of the shape (and by fitting the ratio a_f/a_n also of the absolute value) of the nuclear fissility as a function of E^* only for low values of E^*. Cherepanov and Iljinov's [48] and Iljinov, Mebel's *et al.* [28] systematics for $a(Z, N, E^*)$ allow one to obtain a good description of the data in a larger interval of E^*, they reproduce very close results and seem to describe the data better than the popular systematics of Ignatyuk *et al.* [49].

IV. THE FISSION CROSS-SECTION

In this section, we combine all the above-considered systematics for fission barriers, shell and pairing corrections, level density parameters, and formulae for the calculation of the fission width in the Cascade-Exciton Model (CEM) of nuclear reactions [51] and calculate the fission cross-section for intermediate-energy proton-induced reactions. As the details may be found in [51], we remember here only that the model assumes that the reactions occur in three stages. The first stage is the intranuclear cascade, in which primary particles can be rescattered several times

prior to their absorption, or escape from the nucleus. The excited residual nucleus formed after the emission of the cascade particles determines the particle-hole configuration that serves as a starting point for the second, pre-equilibrium stage of the reaction. The subsequent relaxation of the nuclear excitation is treated in terms of the exciton model of pre-equilibrium decay, which includes the description of the equilibrium evaporative stage of the reaction. The model uses the Monte Carlo method to simulate all three stages of the reactions.

The fission cross-section σ_f is determined by the ratio of the number N_f of fission events to the total number N_t of Monte Carlo simulations in CEM,

$$\sigma_f = \sigma_{in} P_f = \sigma_{in} \frac{N_f}{N_{in}} = \sigma_{geom} \frac{N_f}{N_t} , \qquad (37)$$

where $\sigma_{in} = \sigma_{geom} N_{in}/N_t$ is the total reaction cross-section, N_{in} is the total number of simulated inelastic interactions, and σ_{geom} is the geometrical cross-section for the projectile-target interaction. In the case of low-fissioning nuclei (e.g. gold) $N_f << N_t$, and, as a consequence, a large number of cascades should be calculated to obtain the value σ_f with sufficient statistical accuracy, so that the calculation of σ_f becomes extremely time-consuming. Therefore, besides the direct calculation of the fission cross-section via the expression (37), we have carried out (following Barashenkov *et al.* [30]) Monte Carlo sampling by means of the statistical functions $W_n = \prod_{i=1}^{N} w_{ni}$ and $W_f = 1 - W_n$ in this case. Here, W_n is the probability of the nucleus to "drop" the excitation energy E^* by a chain (cascade) of N successive evaporations of particles; W_f is the probability for the nucleus to fission at one of the chain stages; $w_{ni} = 1 - w_{fi}$ is the probability of particle emission at the i-th stage of the evaporative cascade; w_{fi} is the corresponding fission probability which is easy to determine using the formulae (34-35) for the widths Γ_j and Γ_f. After the subsequent averaging of W_f over the total number N_{in} of the cascades followed, and after multiplication of the result by the corresponding total inelastic cross-section σ_{in}, we obtain the following expression for the fission cross-section:

$$\sigma_f = \frac{\sigma_{in}}{N_{in}} \sum_{i=1}^{N_{in}} (W_f)_i . \qquad (38)$$

As an example, the incident energy dependences of experimental and calculated within this formula fission cross-sections for proton-gold and -uranium interactions are shown in Fig. 15. We performed these calculations with Cameron's [18] shell and pairing corrections, third Iljinov, Mebel's *et al.* [23] systematics form the level density parameter, Krappe, Nix and Sierk's [14] fission barriers with the dependences $B_f(E^*)$ proposed by Barashenkov *et al.* [30], by Sauer *et al.* [34], as well as without a dependence of B_f on E^*. The values used for the ratio a_f/a_n are shown in the Figure. One can see that CEM reproduces correctly the shape and the absolute value of the fission cross-sections in the interval of bombarding energies regarded here by choosing the corresponding values for the ratio a_f/a_n, independently of the form of the dependence $B_f(E^*)$ used in the calculations. Similar results have been obtained also for other targets. A more detailed analysis of fission processes in the framework of the CEM will be done in a separate paper.

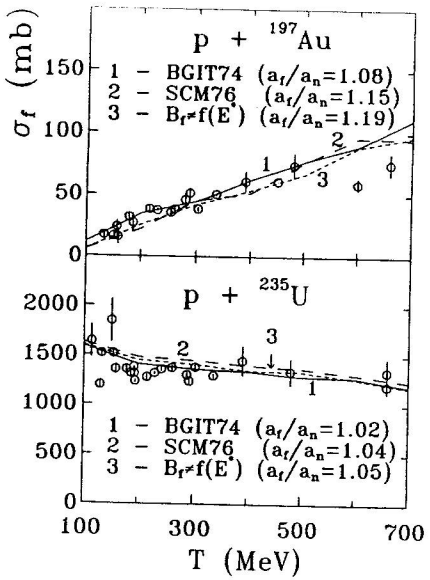

Fig. 15. The energy dependence of the fission cross section for nuclei of gold and uranium. Calculations were performed with KNS79 [14] fission barriers, Cameron's [18] shell and pairing corrections, third Iljinov, Mebel's *et al.* [23] systematics for the level density parameter, for the dependences of B_f on E^* proposed by Barashenkov *et al.* (BGIT74) [30], by Sauer *et al.* (SCM76) [31], as well as without the dependence of B_f on E^*. The values used for the ratio a_f/a_n are shown in the Figure. The experimental points are taken from the summary Table 159 of the monograph [52].

V. SUMMARY AND CONCLUSIONS

Review and comparative analysis of the models for description of fast-computing single-humped fission barriers for statistical calculations are given. It shows that the simple and time-saving phenomenological approaches of Barashenkov *et al.* [16, 17] provide equally good descriptions of the experimental fission barriers with Cameron's [18] and Truran, Cameron and Hilf's [19] shell and pairing corrections both very convenient for Monte Carlo calculations. Nevertheless, for neutron-rich and neutron-deficient nuclei, the use of the shell corrections from Ref. [19] seems to be more preferable. When one uses popular Myers and Swiatecki's [7] shell corrections to describe nuclear fission, the Yukawa-plus-exponential modified LDM [14] provides the best agreement of calculated B_f with the experimental data for the nuclei along the line of β-stability.

Our estimation of the reduction of the fission barrier heights with increasing excitation energy E^* has shown that the phenomenological approach (27) proposed by Barashenkov *et al.* [30] provides a significantly stronger decrease of B_f with increasing E^* in comparison with the approach (25) of Sauer *et al.* [31]. "Thermal" effects may cause about a tenfold increase of the nuclear fissility for medium weight and light nuclei with the excitation energies above 50 MeV.

It has been shown that if one takes into account the dependence of fission barriers on the angular momentum of a fissioning nucleus, the phenomenological approach with formulae (28-30) provides results similar to those obtained by Mustafa's *et al.* [10] and Sierk's [15] models, but needs about one tenth of computing time in comparison with the subroutine BARFIT of Sierk and, therefore, it is more convenient for Monte Carlo calculations. The moments of inertia of Strutinsky [43] at the saddle-point are very close to the Cohen and Swiatecki's [21] ones, so that concrete numerical calculations may be done with any of them.

Nuclear fissilities P_f for different excited compound nuclei as functions of the excitation energies E^* have been studied. We performed a detailed analysis of the dependence of theoretical fissilities on the models for B_f and functional forms $B_f = B_f(E^*)$ and $B_f = B_f(L)$ on the systematics for the level density parameter, and on the values of the ratio a_f/a_n used in the calculations. It has been found that it is possible to select a concrete model for B_f, $a(Z, N, E^*)$, for the shell and pairing corrections, and to fit the ratio a_f/a_n to obtain excellent description of experimental data for every nuclide. But we did not succeed to describe well the experimental P_f simultaneously for all the nuclides with a fixed set of these options. Theoretical values of P_f are the most sensitive ones to the values of the ratio a_f/a_n used in calculations. We have found out that Cherepanov and Iljinov's [48] and Iljinov, Mebel's *et al.* [23] systematics for $a(Z, N, E^*)$ allow one to obtain a good description of nuclear fissilities in the whole interval of excitation energies regarded here, they reproduce results very close and they seem to describe the data better than the popular systematics of Ignatyuk *et al.* [49].

is able to reproduce correctly the shape and the absolute value (let us recall that the CEM predicts the absolute values for all calculated characteristics and does not require any normalization to adjust the results) of the fission cross-sections for proton-nucleus interactions at intermediate energies. This fact, together with good description of proton- and neutron-induced particle production published in [51, 53] indicates the predictive power of CEM and the possibility of using it to provide nuclear data at intermediate energies needed for different important applications, e.g., for the transmutation of long-lived radionuclides produced in reactors with a spallation source.

Our analysis has shown that very voluminous but uncoordinated experimental data on fission processes obtained by now in separate measurements do not permit one to discriminate various models for fission barriers and to determine simultaneously the value of the ratio a_f/a_n. New complex data on fission processes, measured simultaneously with the characteristics of all emitted particles and fragments for such reactions where the fission cross-section is of the same order of magnitude with the particle- and fragment-production cross-sections, and the analysis of all these data in a unique approach may clear up these questions. Such "complete" measurements are possible and desirable in the near future at the FOBOS setup at the Flerov Laboratory of Nuclear Reactions of the Joint Institute for Nuclear Research (Dubna).

REFERENCES

[1] A.V. Ignatyuk, G.N. Smirenkin, M.G. Itkis, S.I. Mulgin and V.N. Okolovich: Fiz.

Elem. Chastits At. Yadra *16* (1985), 709.

[2] L.N. Androneńko, L.A. Vaishnene, A.A. Kotov, M.M. Nesterov, N.A. Tarasov and V. Neubert: Fiz. Elem. Chastits At. Yadra *18* (1987), 685.

[3] M.G. Itkis, V.N. Okolovich, A.Ya. Rusanov and G.N. Smirenkin: Fiz. Elem. Chastits At. Yadra *19* (1988), 701.

[4] J.O. Newton: Fiz. Elem. Chastits At. Yadra *21* (1990), 821.

[5] A. Michaudon: Invieted talk presented at the Workshop on Computation and Analysis of Nuclear Data Relevant to Nuclear Energy and Safety (ICTP, Trieste, Italy 10 February - 13 March 1992), H4.SMR/614/18, Trieste, 1992.

[6] J.F. Berger, M. Girod and D.Gogny: Nucl.Phys. *A502* (1989) 85c.;
V.V. Pashkevich: Proc. Int. Sch.-Sem. on Heavy Ion Phys., Dubna, 1983, p. 405;
P. Möller and J.R. Nix: Nucl. Phys. *A229* (1974) 269;
U. Mosel: Phys. Rev. *C6* (1972) 971.

[7] W.D. Myers and W.S. Swiatecki: Ark. Fyz. *36* (1967), 343.

[8] H.C. Pauli and T. Ledergerber: Nucl. Phys. *A175* (1971), 545.

[9] S. Cohen, F. Plasil and W.J. Swiatecki: Ann. Phys. (N.Y.) *82* (1974), 557.

[10] M.G. Mustafa, P.A. Baisden and H. Chandra: Phys. Rev. *C25* (1982), 2524.

[11] R.W. Hasse: Ann. Phys. (N.Y.) *68* (1971), 377.

[12] W.D. Myers: Droplet Model of Atomic Nuclei (IFI/Plenum, New York, 1977).

[13] H.J. Krappe and J.R. Nix: Proc. 3rd IAEA Symp. on the Phys and Chemistry of Fission, Rochester, New York, 1973 (IAEA-SM-174/12, Vienna, 1974), v.1, p. 159.

[14] H.J. Krappe, J.R. Nix and A.J. Sierk: Phys. Rev. *C20* (1979), 992.

[15] A.J. Sierk: Phys. Rev. *C33* (1986), 2039.

[16] V.S. Barashenkov, A.S. Iljinov, V.D. Toneev and F.G. Gereghi: Nucl. Phys. *A206* (1973), 131.

[17] V.S. Barashenkov and F.G. Gereghi: Communication JINR, P4-10781, Dubna, 1977.

[18] A.G.W. Cameron: Can. J. Phys. *35* (1957), 1021.

[19] J.W. Truran, A.G.W. Cameron and E. Hilf: Proc Int. Conf. on the Properties of Nuclei Far From the Region of Beta-Stability, Leysin, Switzerland, 1970, v. 1, p. 275.

[20] V.E. Viola and B.D. Wilkins: Nucl. Phys. *82* (1966), 65.

[21] S. Cohen and W.J. Swiatecki: Ann. Phys. (N.Y.) *22* (1963), 406.

[22] A.V. Ignatyuk, M.G. Itkis, I.A. Kamenev, S.I. Mulgin, V.N. Okolovich, Yu.B. Ostapenko and G.N. Smirenkin: Yad. Fiz. *40* (1984), 1404.

[23] A.S. Iljinov, M.V. Mebel, N. Bianchi, E. De Sanctis, C. Guaraldo, V. Lucherini, V. Muccifora, E. Polli, A.R. Reolon and P. Rossi: Nucl. Phys. *A543* (1992) 517.

[24] V.M. Kuprianov, K.K. Istekov, B.I. Fursov and G.N. Smirenkin: Yad. Fiz. *32* (1980), 355.

[25] M. Dahlinger, D. Vermeulen and K.-H. Schmidt: Nucl. Phys. *A376* (1982), 94.

[26] S. Bjørholm and J.E. Lynn: Rev. Mod. Phys. *52* (1980), 725;
B.S. Bhandari and Y.B. Bendardaf: Phys. Rev. *C45* (1992), 2803;
B.S. Bhandari: Phys. Rev. *C42* (1990), 1443.

[27] J.R. Nix: Nucl. Phys. *A130* (1969), 241.

[28] A.E.S. Green: *Nuclear Physics* (Mc Graw–Hill, New York, 1955), pp. 185, 250.

[29] U. Mosel and H.W. Schmitt: Phys. Lett. *B37* (1971) 335;
G.M. Raibeck and J.W. Coblle: Phys. Rev. *153* (1965) 1270;
L.G. Moretto, S.G. Tompson, J. Routti and R.C. Gatti: Phys. Lett. *B38* (1972) 471;
P.E. Vorotnikov, Z.S. Gladkih, A.V. Davidov, S.M. Dubrovina, G.A. Otroshenko, E.S. Palshin, V.A. Shigin and V.M. Shubko: Yad. FiZ. *16* (1972) 916;
D. Turck, W. Ziga and H.G. Clerc: Phys. Lett. *B48* (1974) 333; ibid, *B63* (1976) 283;
A.V. Ignatuk, M.G. Itkis, V.N. Okolovich, G.N. Smirenkin and A.S. Tishin: Yad. Fiz. *21* (1975) 1185;
H.L. Pai and D.G. Andrews: Can. J. Phys. *54* (1976) 2056.

[30] V.S. Barashenkov, F.G. Gereghi, A.S. Iljinov, and V.D. Toneev: Nucl. Phys. *A222* (1974), 204.

[31] G. Sauer, H. Chandra and U. Mosel: Nucl. Phys. *A264* (1976), 221.

[32] R.W. Hasse and W. Stocker: Phys. Lett. *B44* (1973), 26.

[33] M. Pi, X. Vinas and M. Barranco: Phys. Rev. *C26* (1982), 733.

[34] J. Bartel and P. Quentin: Phys. Lett. *B152* (1985), 29.

[35] Y. Yamaguchi: Prog. Theor. Phys. *6* (1951), 529.

[36] J.O. Newton, D.G. Popescu and J.R. Leigh: Phys. Rev. *C42* (1990), 1772.

[37] F. Garcias *et al.*: Nucl. Phys. *A495* (1989), 169c; Phys. Rev. *C40* (1989), 1522; Z. Phys. *A336* (1990), 31.

[38] A.S. Iljinov, E.A. Cherepanov, S.E. Chigrinov and S.G. Mashnik: Preprint INR AS USSR, P-0156, Moscow, 1980.

[39] F. Saint-Laurent, M. Conjeaud, R. Dayras, S. Harar, H. Oeschler and C. Volant: Nucl. Phys. *A422* (1984), 307.

[40] M. Beckerman and M. Blann: Phys. Lett. *B68* (1977), 31; Phys. Rev. *C17* (1978), 1615.

[41] F. Plasil, R.L. Ferguson, R.L. Hahn, F.E. Obenshain, F. Pleasonton and G.R. Young: Phys. Rev. Lett. *45* (1980), 333.

[42] E.A. Cherepanov: Proc. Int. Symp. on In-Beam Nuclear Spectroscopy, Debercen, Hungary, May 14 – 18, 1984, p.499.

[43] V.M. Strutinsky: Yad. Fiz. *1* (1965), 821.

[44] V.Weisskopf: Phys. Rev. *52* (1937), 295.

[45] N. Bohr and J.A. Wheeler: Phys. Rev. *56* (1939), 426.

[46] I. Dostrovsky: Phys. Rev. *111* (1958), 1659;
I. Dostrovsky, Z. Fraenkel and G. Friedlander: Phys. Rev. *116* (1959), 683.

[47] A.S. Iljinov, E.A. Cherepanov and S.E. Chigrinov: Yad. Fiz. *32* (1980), 322.

[48] E.A. Cherepanov and A.S. Iljinov: Nucleonika *25* (1980), 611; Preprint INR AS USSR, P-0064, Moscow, 1977.

[49] A.V. Ignatyuk, G.N. Smirenkin and A.S. Tishin: Yad. Fiz. *21* (1975), 485.

[50] A.V. Malyshev: *Level Density and Structure of Atomic Nuclei.* Atomizdat, Moscow, 1969.

[51] K.K. Gudima, S.G. Mashnik and V.D. Toneev: Nucl. Phys. *A401* (1983), 329.]

[52] V.S. Barashenkov and V.D. Toneev: *Interaction of High Energy Particle and Nuclei with Atomic Nuclei.* Atomizdat, Moscow, 1972.

[53] V.I. Komarov *et al.*: Nucl. Phys. *A326* (1979), 297;
S.G. Mashnik and S. Tesch: Z. Phys. *A312* (1983), 259;
S.G. Mashnik: in: Proc. 18th Winter School Leningrad Inst. Nucl. Phys., vol. 3 (Leningrad, 1983) p. 172;
S.G. Mashnik, S. Tesch and S.V. Dzemuhadze: Preprint Inst. Appl. Phys. 84-3, Kishinev (1984);
V.N. Baturin *et al.*: Preprint LINP-1302, Leningrad (1987)
S.G. Mashnik: JINR Preprint E2-92-320, Dubna, 1992 (submited to Nucl. Phys. A).